Ion Transfer Voltammetry Associated with Two Polarizable Interfaces Within Water and Moderately Hydrophobic Ionic Liquid Systems

Shiyu Gan,[a, b] *Min Zhou*,[a] *Jingdong Zhang*,[b] *Lijie Zhong*,[a] *Jens Ulstrup*,[b] *Li Niu**[a, b]

[a] Engineering Laboratory for Modern Analytical Techniques, c/o State Key Laboratory of Electroanalytical Chemistry, Changchun, Institute of Applied Chemistry, and Graduate University of the Chinese Academy of Sciences, Chinese Academy of Sciences, Changchun 130022, P. R. China
tel: +86 431 85262425, fax: +86 431 85262800.
[b] Department of Chemistry and Nano DTU, Technical University of Denmark, DK-2800 Kgs, Lyngby, Denmark
*e-mail: lniu@ciac.jl.cn

Abstract

An electrochemical system composed of two polarizable interfaces (the metallic electrode|water and water|ionic liquid interfaces), namely two-polarized-interface (TPI) technique, has been proposed to explore the ion transfer processes between water and moderately hydrophobic ionic liquids (W|mIL), typically 1-octyl-3-methylimidazolium bis(trifluoromethylsulfonyl)imide ($C_8mimC_1C_1N$) and 1-hexyl-3-methylimidazolium bis(trifluoromethylsulfonyl)imide ($C_6mimC_1C_1N$). Within the classic four-electrode system, it is not likely that the ion transfer information at the W|mIL interface can be obtained due to an extremely narrow polarized potential window (ppw) caused by these moderately hydrophobic ionic components. In this article, we show that TPI technique has virtually eliminated the ppw limitation based on a controlling step of concentration polarization at the electrode|water interface. With the aid of this technique, the formal ion transfer potential differences between $C_1C_1N^-$ and C_nmim^+ ($n = 6, 8$) were accurately determined for 356 mV and 420 mV at a corresponding interface (W|$C_6mimC_1C_1N$ and W|$C_8mimC_1C_1N$). Besides, this technique is used to monitor electrochemical polarization at the two W|mIL systems, which exhibits an adaptable polarizability (i.e., a conversion from a nonpolarized interface to a polarized interface). Some of the typical anion transfers at the W|$C_8mimC_1C_1N$ interface have also been investigated, as they are particularly important for ion extraction. The experimental results indicate that this facile TPI technique offers a general avenue to explore ion transfer in multifarious biphasic systems.

1 Introduction

In the technical development of liquid|liquid (L|L) interface electrochemistry, the first historical example of the classic four-electrode system pioneered by Samec and co-workers has tremendously improved the charge transfer studies at the interface between two immiscible electrolyte solutions (ITIES) [1]. Hitherto, this technique is the most widely used electrochemical device for exploring the interfacial electron transfer (ET) and ion transfer (IT) at various biphasic systems. Another important method can be ascribed to the micro-interface technique introduced by Taylor and Girault, by which IT kinetic information could be obtained due to the efficient mass transfer coefficients [2]. This micro-L|L interface technique was further developed to an array form for an enhanced current signal, providing a new soft interface sensitive platform for detecting ions and even biomolecules [3]. Moreover, recently reported smaller nanoscopic L|L interfaces exhibites more efficient mass transfer and low back ground current resulting in IT kinetic determination even in low polarity *n*-octanol [4] and high viscosity ionic liquids [5].

The above mentioned techniques can be essentially summarized as a single-polarized-interface (SPI) electrochemical system, that means only one interface (e.g., water|oil (W|O) or water|ionic liquid (W|IL)) is polarized during the voltammetric process. An inherent problem for the SPI system is the polarized potential window (ppw) limitation caused by the supporting electrolyte ionic components in the adjoining two phases, which indicates that charge transfer studies should be located in the ppw. Another innovative strategy is the liquid-droplet or liquid-film technique, in which the L|L interface is constructed from a small volume of water or oil phase supported by a solid electrode (e.g., Pt or carbon electrode). The basis is ET studies at the interface between a very thin organic layer and water phase which was first pro-

posed by Anson and co-workers [6]. Along this line, a water-droplet biphasic system constituted by two serial interfaces (e.g., Pt|W and W|O) has been provided to explore the IT behavior [7]. The great advantages of this technique are manifested in three aspects: (i) it is an alternative to a classic four-electrode potentiostat owing to its simple three-electrode setup; (ii) compared to an individual ET or IT process in the four-electrode system, the electrochemical process is an essential ET coupled IT reaction (ET-IT), which provides other insight to probe IT studies; (iii) a large difference of phase ratio can give a fast equilibrium between the two liquid phases. Besides, this water-droplet approach has recently shown an interesting characteristic of completely removing ions from water to the oil phase which could be used as a new system in calibration-free coulometric ion sensing [8]. Nevertheless, these reported water-droplet technique still belonges to a SPI system due to a nonpolarized interface characteristic between supporting solid electrode and water phase in terms of their electrochemical cell design.

Inspired by the water-droplet approach and the ET-IT coupled mechanism [7], a modified method, namely two-polarized-interface (TPI) technique has been first proposed in our previous work [9]. This TPI system is also composed of two serial interfaces (Pt|W and W|O), while special experimental cell design brings about a polarized Pt|W interface and especially the determining step of mass transfer in ET process. This method has been successfully applied to determine the Gibbs transfer energies of almost total extremely hydrophilic supporting electrolyte ions [9a] and even heavy-metal ions [9b] at the water|1,2-dichlorethane (W|DCE) interface. The experimental results have confirmed that this TPI technique as an effective strategy can resolve the ppw limitation. Analogously, based on the similar ET-IT reaction mechanism, other liquid-droplet systems involving oil droplets [10], oil films [11] and three-phase junctions [12] also make great progress, such as, offering a new method for kinetic measurement [11] and determining the partition coefficients of drugs in the *n*-octanol|water system [12d]. Challenges still exist including the rigorous hydrophobic requirements of redox probes and the side effects between the probes and transferring ions [13].

With regard to traditional water|molecular organic solvents system, a new biphasic media of water|hydrophobic ionic liquid interfaces, has recently attracted considerable interest because of its special interfacial characteristics (e.g., electrical double layer structure [14], ultraslow relaxation [14c,15] and interfacial adsorption [14a,16]), and moreover its foreseen practical applications (e.g., ion extraction [17], compound separation [18], biocatalysis [19] and electrochemical devices [20]). Most of IT studies at W|IL interfaces have focused on the SPI system including four-electrode [14], single [21] and array micro-interfaces [22]. Quinn et al. first employed IT voltammetry with a micropipette technique [21a]. Unfortunately, this could not be accomplished due to the limitation of ppw (<50 mV) caused by the not strongly hydrophobic ionic

compositions. To account for this problem, numerous strongly hydrophobic ionic liquids such as BEHSS- and TPFB-based [23,24a,b] and recently reported asymmetric hydrophobic room temperature ionic liquids (e.g., [H3DA][TPBF20]) [23,24c] reveal a wider ppw, thereby leading to the possibility to study several moderately hydrophobic and hydrophilic ion transfers [25]. However, the transfer for supporting electrolyte ions in water (e.g., Li^+ and Cl^-) [24a] and IL phases (the ionic components constituting IL) [24b], still cannot be accurately assessed due to the inherent problem of ppw limitation in SPI system.

In this study, to overcome the ppw limitation problem, we use our TPI technique to explore the IT process at two typical water|moderately hydrophobic ionic liquid (W|mIL) systems, 1-octyl-3-methylimidazolium bis(trifluoromethylsulfonyl)imide ($C_8mimC_1C_1N$) and 1-hexyl-3-methylimidazolium bis(trifluoromethylsulfonyl)imide ($C_6mimC_1C_1N$). We first give a detailed illustration of the TPI concept and its great advantages. We then combine sensitive square wave voltammetry (SWV) technique to study the electrochemical polarization process and the transfer of ionic components constituting the mIL at the two W|mIL interfaces. Finally, the most important anion insertions from W to mIL are measured.

2 Experimental

2.1 Reagents

1-Octyl-3-methylimidazolium bis(trifluoromethyls-ufonyl)-imide ($C_8mimC_1C_1N$, 99.9%), 1-hexyl-3-methylimidazolium bis(trifluoromethylsulfonyl)imide ($C_6mimC_1C_1N$, 99.9%) and bis(trifluoromethylsulfonyl)imide lithium (LiC_1C_1N, 99.9%) were purchased from the centre for Green Chemistry and Catalysis, Lanzhou Institute of Chemical Physics (LICP). $K_4Fe(CN)_6$, $K_3Fe(CN)_6$, KCl, NaCl, $NaPF_6$, $NaBF_4$, NaSCN, $NaIO_3$, $NaBrO_3$, $NaClO_3$, $NaNO_3$, CH_3COONa (NaAc) and NaF were bought from Beijing Chemical Co., China. All chemicals of analytical grade were used as received. All aqueous solutions were prepared with deionized water (Milli-Q, Millipore).

2.2 Instruments, Electrodes and Procedures

Voltammetric experiments including cyclic voltammetry (CV) and square wave voltammetry (SWV) were undertaken in a conventional three-electrode cell with a CHI660A electrochemical workstation (CH Instruments Inc., Shanghai) with IR compensation. The SWV parameters were: frequency $f = 50$ Hz, amplitude $A = 25$ mV and potential increment $\Delta E = 4$ mV. The micropipette ($d \approx 35$ μm) was fabricated from borosilicate glass capillaries ($o.d./i.d. = 1.0/0.58$ mm, $L = 10$ cm) by using a puller (Model P-97, Sutter Instrument Co.). Appropriate pulling parameters were chosen carefully to make pipettes with short shanks in order to minimize the IR drop. The pipette was filled with the aqueous solution from the back

using a small syringe (10 μL). A drop of 0.5 μL aqueous solution containing an equal molar ratio of the redox couple was transferred to the surface of a freshly polished platinum disk electrode ($d = 1$ mm) with a small syringe, which spreads spontaneously across the surface and covers it completely. Then it was turned over and immersed immediately into water-saturated ionic liquids (1.0 mL). All the measurements are performed at room temperature.

3 Results and Discussion

3.1 Comparisons of IT Voltammetry at the W|mIL Interfaces with Two Polarizing Manners
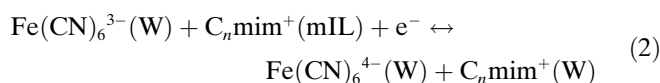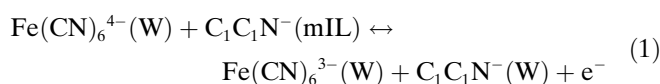
Scheme 1a shows a three-electrode setup for the W|mIL biphasic systems supported on a microscopic L|L interface. It is a typical SPI setting, in which only the W|mIL interface would be polarized during the voltammetric process. The electrochemical cell configuration (Scheme 1b) composed of two serial interfaces (Pt|W and W|mIL) exhibits a TPI setup. In fact, the concepts of SPI and TPI were first shown in liquid membrane technique [26] and detailed theoretical studies by the Samec [27a] and Molina [27b–d] groups. In their cells, one side of the membrane is polarized in a SPI system whereas both sides are polarized simultaneously in TPI system. Herein, to achieve a target of illustration of the advantage for the TPI technique, two polarizing manners (SPI and TPI systems) would be undertaken to compare the IT behavior at the W|mIL interfaces. Corresponding electrochemical cells are given in Scheme 1c.

Figure 1a and 1b show a familiar ppw for W|C$_6$mimC$_1$C$_1$N and W|C$_8$mimC$_1$C$_1$N interfaces using a SPI system (cell 1). The transfers of C$_1$C$_1$N$^-$ exhibit nearly the same potential (ca. 0 V) in the two W|mIL interfaces when the current level is up to 0.5 μA, while the transfer potential of C$_8$mim$^+$ is more negative (ca. 50 mV) than that of C$_6$mim$^+$, corresponding to the higher hydrophobicity of C$_8$mim$^+$ [28]. The widths of the ppw at the two W|mIL interfaces are estimated to be about 50 mV and 80 mV from the region of no apparent Faradic current in the CVs (Figure 1a and 1b). In such a narrow ppw, it is not possible to evaluate the transfer of available ions or even ionic components constituting the mIL. With respect to ppw-shape transfer of the C$_n$mim$^+$ and C$_1$C$_1$N$^-$ in the SPI system (i.e., ion transfers at the end of ppw), Figure 1c and 1d show two pairs of well-defined current waves using the TPI system (cell 2). In our previous work [9a], the similar TPI cell (i.e., the water droplet involves the same redox couple of Fe(CN)$_6^{3-/4-}$ and sodium salts immersed in oil phase) has been used to explore the transfer of extremely hydrophilic ions (e.g., F$^-$, OH$^-$, PO$_4^{3-}$) at the W|DCE interface. Two couples of distinct voltammetric peaks were also revealed in CV plots, which were identified as an ET-IT process, that is the ET of Fe(CN)$_6^{3-/4-}$ occurring at the Pt|W interface accompanied with ions (e.g., Na$^+$ and Cl$^-$) across the W|DCE in-
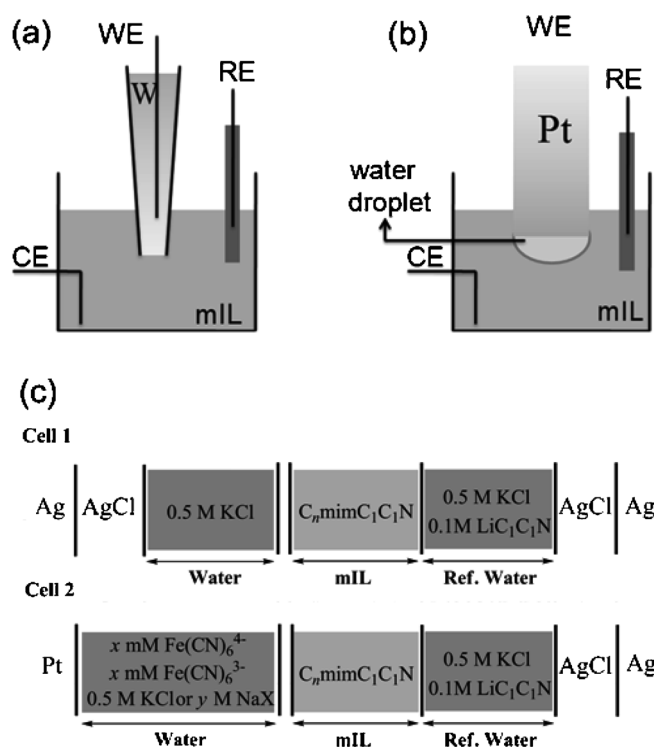
Scheme 1. (a) Schematic presentation of a single-polarized-interface (SPI) electrochemical cell supported on the micropipette ($d \approx 35$ μm). (b) A two-polarized-interface (TPI) electrochemical cell supported on the water droplet modified Pt electrode. (c) Corresponding electrochemical cells for SPI system (cell 1) and TPI system (cell 2). WE: working electrode, RE: reference electrode, CE: counter electrode, mIL: moderately hydrophobic ionic liquid phase, W: water phase, $n = 6, 8$.

terface. As shown in Figure 1c and 1d, the two current waves represent ET-IT processes, in which ion transfers can be ascribed to C$_n$mim$^+$ ($n = 6$, 8) and C$_1$C$_1$N$^-$ due to the highly hydrophilic K$^+$ and Cl$^-$ [28]. The two coupled reactions can be described by

$$Fe(CN)_6^{4-}(W) + C_1C_1N^-(mIL) \leftrightarrow$$
$$Fe(CN)_6^{3-}(W) + C_1C_1N^-(W) + e^- \quad (1)$$

$$Fe(CN)_6^{3-}(W) + C_n mim^+(mIL) + e^- \leftrightarrow$$
$$Fe(CN)_6^{4-}(W) + C_n mim^+(W) \quad (2)$$

The half-wave potential differences of Equation 1 and 2 as shown in Figure 1c and 1d are evaluated as 184 mV and 96 mV at corresponding W|C$_8$mimC$_1$C$_1$N and W|C$_6$mimC$_1$C$_1$N interfaces, i.e., larger than those of 80 mV and 50 mV obtained by the SPI setting (shown in Figure 1a and 1b). Irregular current oscillations occur at relatively low scan rate at the W|C$_8$mimC$_1$C$_1$N interface (Figure 1d), corresponding to the reverse process of Equation 2 (C$_8$mim$^+$ transfers back from W to mIL). Similar phenomenon was observed in the transfer of surface active ions (e.g., C$_n$SO$_3^-$ and C$_7$F$_{15}$COO$^-$) [23,29a–c] and ionized dendrimers [29d] at conventional L|L and W|IL

These are not the final page numbers! ↗↗

interfaces [12a], which is attributed to electrochemical instability caused by a potential-dependent adsorption and desorption of ion surfactants [29–31]. In fact, it has been demonstrated that C_8mim^+ can be adsorbed at the interface between LiCl aqueous solution and $C_8mimC_2C_2N$ [23,32]. Accordingly, the suggestion that C_8mim^+ is adsorbed at the $W|C_8mimC_1C_1N$ interface would be reasonable. It seems that this TPI technique offers a possibility to explore the oscillation process. In terms of the above experimental results, two interesting issues have emerged involving the transformation of IT manifestation from ppw shape (Figure 1 and 1b) to peak shape (Figure 1c and 1d) and enhanced transfer half-wave potential differences.

We first illustrate the first issue of the transformation of IT manifestation in the CVs. Detailed electrochemical processes in SPI and TPI systems are exemplified in Figure 2. Figure 2a displays an ET-IT process in the SPI system where ET occurring at the $AgCl|Ag$ electrode is associated with IT at the $W|mIL$ interface. Although the current flows to the $(AgCl|Ag)|W$ interface, two points determine that this interface can be still considered as a nonpolarized interface. The first is a typical Nernst ET reaction between the $AgCl|Ag$ electrode and Cl^-. The balance cannot easily be broken when the current is not so large. The second is a relatively low current density at the $(AgCl|Ag)|W$ interface due to the great difference of interfacial area between the two interfaces. Therefore, cell 1 in Scheme 1a is a SPI setting and the problem of ppw limitation remains a challenge.

The situation is quite different for the TPI system. The electrochemical process shown in Figure 2b is also an ET-IT reaction while equivalent current density passes through the $Pt|W$ and $W|mIL$ interfaces due to ap-

Fig. 2. Schematic modes of the electrochemical process occurring at SPI (a) and TPI (b) cell systems. ET and IT present electron transfer and ion transfer at the two serial interfaces, respectively. Red and Ox denote the redox species, $K_4Fe(CN)_6$ and $K_3Fe(CN)_6$, respectively.

proaching interfacial areas. It should be also mentioned that another crucial factor can determine the polarizability for the $Pt|W$ interface, that is the concentration difference between the redox species ($Fe(CN)_6^{3-/4-}$) and coupled transferring ions (C_nmim^+ and $C_1C_1N^-$). When the redox species are concentrated, concentration polarization in IT is the controlling step among the whole ET-IT processes. Thus, the potential drop at the $Pt|W$ interface keeps almost unchanged during the voltammetric process, which can still be recognized as a nonpolarized interface. The electrochemical cell in such a case is still a SPI system [7]. However, in our system (cell 2), the concentrations of redox species (100 mM for $Fe(CN)_6^{3-}$ and $Fe(CN)_6^{4-}$) are much smaller than those of the ionic components constituting ionic liquids (2.88 M for C_8mim^+ and $C_1C_1N^-$, 3.17 M for C_6mim^+ and $C_1C_1N^-$, detailed calculations in supporting information (SI)). Apparently, the concentration polarization of ET dominates the entire ET-IT process, thereby causing a varied interfacial concentration of the redox species at the $Pt|W$ interface during the potential scan. This suggests that the potential drop at $Pt|W$ interface is no longer fixed. Meanwhile, the $W|mIL$ is polarized and thus cell 2 is no doubt a TPI system.

In the SPI systems, such as in the four-electrode [1] micropipette technique (Scheme 1a) and initially proposed water-droplet method [7], an inherent problem of ppw limitation cannot be eliminated. Our previous work [9] and the above analysis have demonstrated that a crucial conversion of the controlling step (concentration polarization in ET replacing that in IT) makes this droplet technique become a TPI system and moreover resolves the ppw limitation effectively.
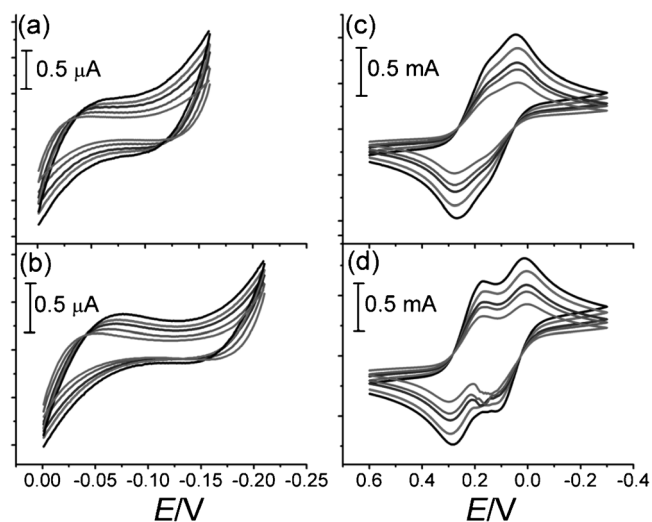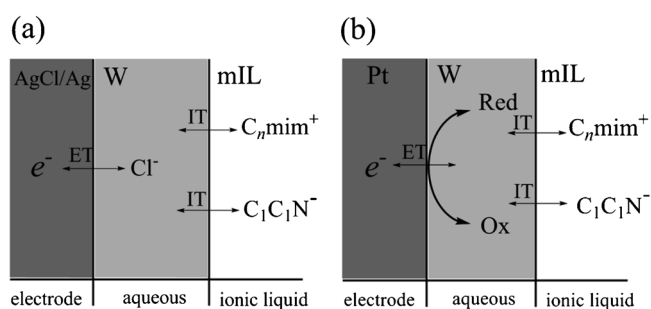

Fig. 1. Cyclic voltammograms (CVs) recorded using cell 1 at the $W|C_6mimC_1C_1N$ (a) and $W|C_8mimC_1C_1N$ (b) interfaces; scan rate: 0.1, 0.2, 0.4, 0.6, 1.0 V s^{-1}. The corresponding CVs obtained using cell 2 ($y=0$) at $W|C_6mimC_1C_1N$ (c) and $W|C_8mimC_1C_1N$ (d) interfaces; scan rate: 0.5, 0.8, 1.0, 1.5, 2.0 V s^{-1}. The scan proceeds from positive to negative potential.

3.2 Electrochemical Polarization at the W|mIL Interface and the Transfer of Ionic Components Constituting the mIL

The electrochemical polarization in a $W|IL$ biphasic system depends on the hydrophobicity of the IL [33]. For the $W|mIL$ interfaces, the degree of electrochemical po-

larizability is small due to not strongly ionic components [33b, 34]. The experimental results shown in Figure 1a and 1b (an extremely narrow ppw) have confirmed this fact. Kakiuchi has elucidated theoretically and experimentally that the phase-boundary potential for W| $C_8mimC_nC_nN$ ($n = 1, 2$) interface is determined by the partition of the ionic components of this IL, which means a nonpolarized interface property in this W|mIL system [33b]. Recently, some BEHSS- and TPFB-based [23] strongly hydrophobic ionic liquids reveal a wider ppw [24], which have been used to explore the IT [25a, 26a], facilitated IT [25b, 26b, 35] and even voltammetric determination of K^+ and Na^+ in tap water samples [26b]. Indeed, there was no demarcation line that divided the two types of interfaces (polarized and nonpolarized). Using the TPI electrochemical system and sensitive SWV technique, we can monitor the electrochemically polarized process at W|mIL interfaces and provide a new strategy to quantitatively measure the polarizable degree of the W|mIL system. The second issue of enhanced transfer potential differences in the first part is resolved below.

SWVs associated with sequential concentrations of the redox species at the W|$C_8mimC_1C_1N$ and W| $C_6mimC_1C_1N$ interfaces are exemplified in Figure 3. The left and right peaks correspond to Equation 1 and Equation 2, respectively. The apparent half-wave potential ($E_{1/2}$) for the two reactions can be given by Equation 3 and Equation 4 (more detailed derivations could be found in Section 5, Appendix)

$$E_{1/2}(C_1C_1N^-) = \Delta_W^{Pt}\phi^{\Theta'} + \Delta_{IL}^W\phi_{C_1C_1N^-}^{\Theta'}$$
$$-f\ln\left(2\gamma_1K_1 - t_{C_nmim^+}^{IL}\right) + C_1 \tag{3}$$

$$E_{1/2}(C_nmim^+) = \Delta_W^{Pt}\phi^{\Theta'} + \Delta_{IL}^W\phi_{C_nmim^+}^{\Theta'}$$
$$+f\ln\left(2\gamma_2K_2 - t_{C_1C_1N^-}^{IL}\right) + C_2 \tag{4}$$

where $f = F/RT$, K_1 and K_2 denote the bulk concentration ratios between the transferring ions and the redox species (i.e., $C_1C_1N^-/Fe(CN)_6^{4-}$ and $C_nmim^+/Fe(CN)_6^{3-}$), respectively. $\Delta_W^{Pt}\phi^{\Theta'}$ and $\Delta_{IL}^W\phi_j^{\Theta'}$ ($j = C_1C_1N^-$ and C_nmim^+) represent the formal electrode potential of $Fe(CN)_6^{3-/4-}$ and transfer potentials for ionic components of mIL. Other constant parameters (C_1, C_2, γ_1, γ_2, t_j^{IL}) represent the relationships between the diffusion coefficients of the redox species and transferring ions. Their expressions and values can be found in Section 5, Appendix. According to Equation 3 and Equation 4, $\Delta E_{1/2}$ of the anion and cation is given by

$$\Delta E_{1/2} = \Delta_{IL}^W\phi_{C_1C_1N^-}^{\Theta'} - \Delta_{IL}^W\phi_{C_nmin^+}^{\Theta'} - f\ln u + C \tag{5}$$
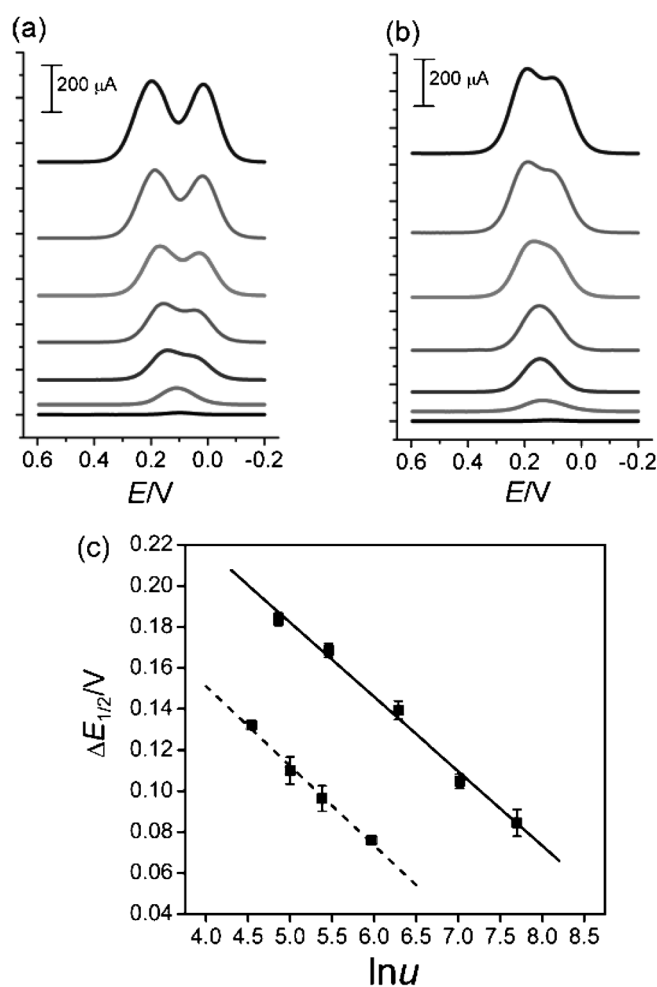
where $C = C_1 - C_2$ and

Fig. 3. SWVs recorded at W|$C_8mimC_1C_1N$ (a) and W| $C_6mimC_1C_1N$ interfaces (b) using cell 2 ($y = 0$), from bottom to top $x = 1, 10, 25, 35, 50, 75, 100$ mM; SWVs were not shown for 120 mM and 150 mM at W|$C_6mimC_1C_1N$ interface. (c) Concentration dependence of the half-wave potential differences between Equation 1 and Equation 2 at W|$C_8mimC_1C_1N$ (solid line) and W|$C_6mimC_1C_1N$ interfaces (dashed line). The meaning of u is given in the text.

$$u = \ln\left(2\gamma_1K_1 - t_{C_nmim^+}^{IL}\right)\left(2\gamma_2K_2 - t_{C_1C_1N^-}^{IL}\right) \tag{6}$$

There is a notable point in Equations 3, 4 and 5 that differentiates the $E_{1/2}$ of IT at the SPI system [1]. $E_{1/2}$ and $\Delta E_{1/2}$ are correlated with K_1 and K_2 that means the IT potential can be modulated by the concentration of redox species. This interesting characteristic would be useful to separate the transfer of ions with close transfer properties. The experimental results shown in Figure 3 have confirmed this expectation. At the W|$C_8mimC_1C_1N$ interface (Figure 3a), only one peak was observed when the concentrations of redox species ($Fe(CN)_6^{3-/4-}$) are 1 mM and 10 mM (i.e., $K_1 = K_2 = 2880, 288$), which indicates that the transfers for C_8mim^+ and $C_1C_1N^-$ cannot be separated. However, the peaks are gradually discernable with the concentration increasing from 25 mM to 100 mM, $\Delta E_{1/2}$ has been raised from 85 mV to 184 mV. The expected

These are not the final page numbers! ↗↗

reason is the concentration dependence of $\Delta E_{1/2}$ (Equation 5). When x is small, such large values of K_1 and K_2 make the $E_{1/2}$ ($C_n$mim$^+$) and $E_{1/2}$ ($C_1C_1N^-$) approach each other ($\Delta E_{1/2}$ decreases to an experimentally indistinguishable value). With the concentration increasing, the decreases of K_1 and K_2 give rise to large $\Delta E_{1/2}$, so that the C_8mim$^+$ and $C_1C_1N^-$ transfers become gradually discriminated. For the W|C_6mimC_1C_1N interface, similar tendency can be seen in Figure 3b. Because of the hydrophobicity of C_6mim$^+$ being smaller than C_8mim$^+$, C_6mim$^+$ and $C_1C_1N^-$ transfers can be separated when the concentration of redox species is up to 75 mM.

The interesting peak-separation process related to concentration variation of redox species strongly suggests a change of electrochemical polarizability at the W|mIL interface. The widths of ppw are only 50 mV and 80 mV for the two W|mIL systems in the SPI cell (Figure 1a and 1b), which implies a small and fixed interfacial polarizability caused by the moderately hydrophobic ionic components. A nonpolarized interface configuration based on a common ion in both phases (e.g., $C_n$mim$^+$ and $C_1C_1N^-$), was developed to study ET [36] and interfacial adsorption [32] at these W|mIL interfaces. With the TPI technique, the polarizability can be modulated by changing the concentration of redox species. When low concentrations are applied (e.g., 1 mM and 10 mM in Figure 3a and 1, 10, 25, 35, 50 mM in Figure 3b), the low current density is insufficient to change the composition of the W|mIL interface, so that the interface in such a case reveals characteristics of a nonpolarized interface, thereby leading to indistinguishable transfer for $C_n$mim$^+$ and $C_1C_1N^-$ (only one peak observed in SWVs). With increasing the concentration, large current density makes the interface polarized and thus the two reactions (Equation 1 and Equation 2) can be distinguished gradually.

Well-defined linear curves shown in Figure 3c further support the concentration dependence in Equation 5. The slope obtained for the respective W|C_8mimC_1C_1N and W|C_6mimC_1C_1N interfaces is −36.3 and −36.8 mV, slightly higher than the theoretical value of −25.9 mV corresponding to the case of large phase ratio [37] (ca. 2000 in our experiments). The intercept of Equation 5 gives the standard transfer potential difference of the ionic liquid components (i.e., the quantitative width of ppw). These values determined for $C_1C_1N^-/C_8$mim$^+$ and $C_1C_1N^-/C_6$mim$^+$ are 420 mV and 356 mV according to the intercept in Figure 3c (detailed calculations in SI). With regard to commonly used semiquantitative methods like linear-scan voltammetry [21a,38] and a quantitative procedure of charge transfer resistance [34], this TPI technique provides a simple and accurate strategy to evaluate the width of the ppw for some unknown biphasic systems.

3.3 Anion Insertion from W to mIL

In recent studies about the IT process at W|mIL interfaces based on IL-redox active drop [39,40], the electrochemical process in their method is also an ET-IT process

while the measured ion species would be restricted owing to the not strong hydrophobicity of electrogenerated redox species (e.g., *t*-butylferrocene cation). With the TPI system, the transfer of supporting electrolyte ions in aqueous media becomes measurable voltammetrically. SWVs for the transfer of several anions across the W|C_8mimC_1C_1N interface are displayed in Figure 4. For BF$_4^-$, BrO$_3^-$ and IO$_3^-$, SWVs are performed in the presence of 0.05 M Fe(CN)$_6^{3-/4-}$ and 0.25 M NaX because of solubility limitation for these sodium salts. Since $E_{1/2}$ (Equation A16) is dependent on the concentration ratio between the redox species and the coupled transferring ions, the same ratio of 0.1 M Fe(CN)$_6^{3-/4-}$ to 0.5 M NaX in other ion measurements is applied for a comparison.

The values of $\Delta E_{1/2}$ between C_8mim$^+$ and $C_1C_1N^-$ shown in Figure 3a are 140 mV and 184 mV for 0.05 M and 0.1 M Fe(CN)$_6^{3-/4-}$, respectively, $E_{1/2}$ of Cl$^-$, Ac$^-$ and F$^-$ (listed in Table 1) equate the maximum value of 184 mV, which indicates that C_8mim$^+$ insertions are preferentially from mIL to aqueous solution. $E_{1/2}$ (Br$^-$) of 177 mV and $E_{1/2}$ (IO$_3^-$) of 136 mV approaching the maximum width reveal that Br$^-$, IO$_3^-$ and C_8mim$^+$ have close transfer potentials. The transfers for PF$_6^-$, BF$_4^-$, SCN$^-$, BrO$_3^-$, NO$_3^-$ and ClO$_3^-$ are within this region. However, it should be noted for the PF$_6^-$ and BF$_4^-$ that their transfer potentials are close to that of $C_1C_1N^-$. Nearly overlapped two peaks for PF$_6^-/C_1C_1N^-$ and BF$_4^-/C_1C_1N^-$ indicate that the W|C_8mimC_1C_1N interface in such a case exhibits an approaching nonpolarized characteristic. Similar results of one peak were observed in Figure 3a and 3b when the concentration of Fe(CN)$_6^{3-/4-}$ is not high enough to polarize the W|mIL interfaces. More concen-
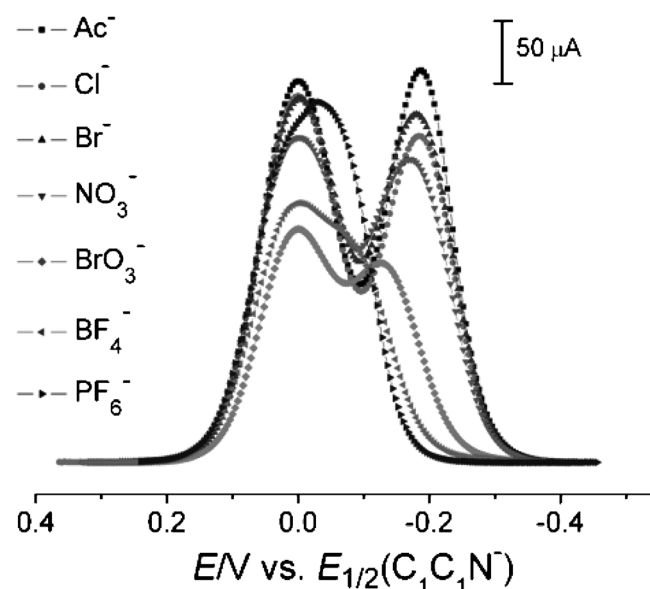

Fig. 4. SWVs recorded using cell 2 for several selected anion transfers across the W|C_8mimC_1C_1N interface. For BF$_4^-$, BrO$_3^-$ and IO$_3^-$ ions, x and y equate 50 mM and 0.25 M, respectively. For other ions, $x = 100$ mM and $y = 0.5$ M. The SWV parameters are the same as in Figure 3.
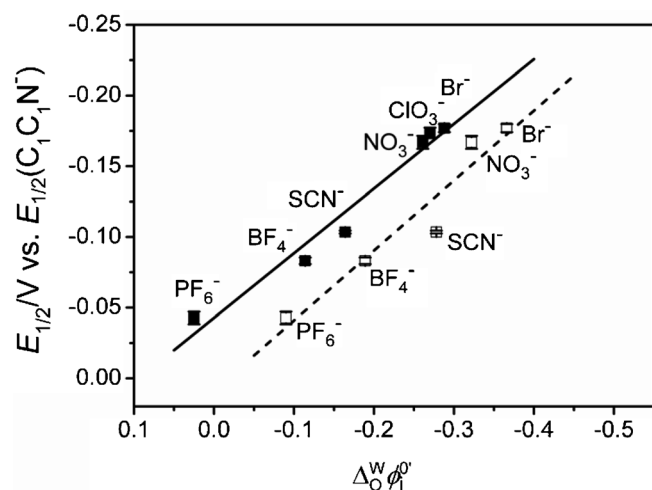
⤢⤢ These are not the final page numbers!

Fig. 5. Correlation of the half-wave potentials for IT across the W|C$_8$mimC$_1$C$_1$N interface with standard IT potentials across the W|DCE (open square) and W|NB (solid square) interfaces. Solid and dashed lines are linear fit to the plots of anions for the two interfaces, respectively.

trated redox species are needed to discriminate the two ion transfers.

For a comparative analysis, Table 1 lists the standard IT potentials across the W|DCE and water|nitrobenzene (W|NB) interfaces. Figure 5 represents the correlation of $E_{1/2}$ with $\Delta_{DCE}^{W}\phi_i^{\ominus'}$ and $\Delta_{NB}^{W}\phi_i^{\ominus'}$. The same tendency indicates that C$_8$mimC$_1$C$_1$N has similar solvation behavior as DCE and NB. Both linear regression slopes of 0.49 for DCE and 0.46 for NB are smaller than unity which shows a higher polarity of C$_8$mimC$_1$C$_1$N. For the W|C$_6$mimC$_1$C$_1$N interface, a challenge of IT still encountered in the width of only 96 mV under 0.1 M Fe(CN)$_6^{3-/4-}$. A new strategy of increasing current density at this interface, by reducing the area of the W|mIL interface, and not by raising the concentration of redox species easily causing an oscillation in high currents, would be an effective strategy to resolve the problem. Further researches on the modulation of interfacial polarizability and discussion of

Table 1. Half-wave potentials at the W|C$_8$mimC$_1$C$_1$N interface and the apparent standard IT potentials at the W|DCE interface and at the W|NB interface.

Ions	$E_{1/2}$ (mV) [a]	$\Delta_{DCE}^{W}\phi_i^{\ominus'}$ (mV) [9a]	$\Delta_{NB}^{W}\phi_i^{\ominus'}$ (mV) [28]
PF$_6^-$	43 ($\pm$5)	-90	25
BF$_4^-$	83 ($\pm$2)	-189	-114
SCN$^-$	104 ($\pm$1)	-278	-164
BrO$_3^-$	124 ($\pm$2)	–	–
IO$_3^-$	136 ($\pm$4)	–	–
NO$_3^-$	167 ($\pm$5)	-322	-261
ClO$_3^-$	174 ($\pm$4)	–	-270
Br$^-$	177 ($\pm$3)	-366	-288
Cl$^-$	183 ($\pm$1)	-470	-396
Ac$^-$	184 ($\pm$7)	-497	–
F$^-$	186 ($\pm$5)	-502	–

[a] $E_{1/2}$ vs. $E_{1/2}$ (C$_1$C$_1$N$^-$)

the nature of the oscillation (Figure 1d) will be focused by this new TPI technique.

4 Conclusions

In conclusion, we have introduced two electrochemical systems (SPI and TPI cells) to explicitly differentiate the CV characteristics of IT at W|mIL interfaces (W|C$_8$mimC$_1$C$_1$N and W|C$_6$mimC$_1$C$_1$N). The transformation of IT pattern from ppw shape (in SPI system) to peak shape (in TPI system) would not only present a strong illustration of the TPI concept, but also offer a general avenue to appraise the transfer of supporting electrolyte ions in both adjoining liquid phases, which indicates that this TPI technique has virtually eliminated the problem of ppw limitations. Moreover, with this TPI technique, some anion insertions from W to mIL have been successfully achieved, which offers an electrochemical strategy to assess ion extraction in W|mIL systems. Furthermore, an interesting peak-separation process modulated by the concentration of redox species further allows us to deepen understanding of the interfacial polarization at W|mIL interface, just like Kakiuchi [34] said "there is no demarcation line that divided polarized and nonpolarized interfaces." Our experiments show that this new technique can be extended to the case of water|strongly hydrophobic ionic liquids systems, which would be instructive for investigating strongly hydrophilic ions such as Li$^+$, Na$^+$, K$^+$ and even heavy metal ions without ionophores needed.

5 Appendix

The detailed derivations of half-wave transfer potentials of the coupled ET-IT reactions (Equations 3 and 4) are shown in this Appendix. Within the IT voltammetry of cation and anion constituting the mIL with TPI cell (cell 2), the electrochemical process is a coupled reaction at the positive and negative terminal of potential scale which can be expressed as below:

$$R(W) + B^-(mIL) \leftrightarrow O(W) + B^-(W) + e^- \qquad (A1)$$

$$O(W) + A^+(mIL) + e^- \leftrightarrow R(W) + A^+(W) \qquad (A2)$$
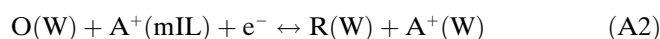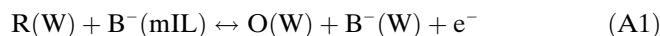
where O, R, A$^+$ and B$^-$ denote Fe(CN)$_6^{3-}$, Fe(CN)$_6^{4-}$, C$_n$mim$^+$ and C$_1$C$_1$N$^-$, respectively. Since the ET and IT processes occur at the two separated interfaces (Pt|W and W|mIL) simultaneously (Figure 2b), we will derive the expressions of current-potential response at the two interfaces, respectively. The bridge connecting ET and IT is equivalent current and electroneutrality condition in both phases. By convention, using Laplace transform, the convolution theorem and flux balance at the Pt|W interface, the convolution $I(t)$ can be given by

These are not the final page numbers! ↗↗

$$\frac{I(t)}{FA_1} = \frac{mC_R^{W,*} - C_O^{W,*}}{(\xi + m)} (\pi D_R^W)^{1/2} \tag{A3}$$

with

$$\left.\begin{array}{l} I(t) = \int_0^t i(\tau)(t - \tau)^{-1/2} d\tau \\ m = \exp[f(\Delta_W^{Pt}\phi - \Delta_W^{Pt}\phi^{\Theta'})] \end{array}\right\} \tag{A4}$$

where t is time, $\Delta_W^{Pt}\phi^{\Theta'}$ is the formal potential of the redox couple, D_R^W, D_O^W, $C_R^{W,*}$ and $C_O^{W,*}$ are the diffusion coefficients and bulk concentrations of the redox species. A_1 is the surface area of Pt|W interface. $\xi = (D_R^W/D_O^W)^{1/2}$ and $f = F/RT$. For the W|mIL interface, accounting for electromigration, the convolution $I(t)$ can be given by

$$\frac{I(t)}{FA_2} = -\frac{C^{IL,*}(q - p)}{pq + t_{B^-}^{IL} q + t_{A^+}^{IL} p} (\pi D^{IL})^{1/2} \tag{A5}$$

with

$$\left.\begin{array}{l} p = (D^{IL}/D_{A^+}^W)^{1/2}\exp[f(\Delta_{IL}^W\phi - \Delta_{IL}^W\phi_{A^+}^{\Theta'})] \\ q = (D^{IL}/D_{B^-}^W)^{1/2}\exp[-f(\Delta_{IL}^W\phi - \Delta_{IL}^W\phi_{B^-}^{\Theta'})] \end{array}\right\} \tag{A6}$$

and

$$\left.\begin{array}{l} D^{IL} = 2D_{A^+}^{IL} D_{B^-}^{IL}/(D_{A^+}^{IL} + D_{B^-}^{IL}) \\ t_{A^+}^{IL} = D_{A^+}^{IL}/(D_{A^+}^{IL} + D_{B^-}^{IL}), \ t_{B^-}^{IL} = 1 - t_{A^+}^{IL} \end{array}\right\} \tag{A7}$$

where $C^{IL,*}$ is the bulk concentrations of mIL, $\Delta_{IL}^W\phi_j^{\Theta'}$ and D_j^W are the formal transfer potentials of j ion ($j = A^+$, B^-) and diffusion coefficients in water. A_2 is the surface area of the W|mIL interfaces. Equation A5 derived in terms of convolution theorem has a similar form as based on sampled-current derivations (similar derivations can be found in [41]). The following discusses the relationship between Equation A3 and Equation A5. Herein, we assume the $A_1/A_2 \approx 1$ in our experiments as only 0.5 μL water droplet is located on the surface of Pt. The external applied potential E can be present,

$$E = \Delta_W^{Pt}\phi + \Delta_{IL}^W\phi - E_{Ref}^{IL} \tag{A8}$$

where $\Delta_W^{Pt}\phi$ and $\Delta_{IL}^W\phi$ are the potential drops at the corresponding interface. E_{Ref}^{IL} is the reference potential in mIL. When the applied potential E is strong positive and negative, i.e., at the positive or negative terminal of the potential scale, the Equation A5 can be reduced to

$$\frac{I(t)}{FA_2} = \frac{C^{IL,*}}{(q + t_{A^+}^{IL})} (\pi D^{IL})^{1/2} \tag{A9}$$

$$\frac{I(t)}{FA_2} = \frac{C^{IL,*}}{(p + t_{B^-}^{IL})} (\pi D^{IL})^{1/2} \tag{A10}$$

As noted by Kakiuchi and Senda [41], the error cannot exceed 1% using Equation A9 and Equation A10 to replace Equation A5 even when $\Delta_{IL}^W\phi_{B^-}^{\Theta'} - \Delta_{IL}^W\phi_{A^+}^{\Theta'} = 0.1$ V. Therefore, we will use the approximate expressions of Equation A9 and Equation A10 to derive the half-wave transfer potentials ($E_{1/2}$) of coupled reactions, Equation A1 and Equation A2. Since the concentrations of the redox couple is far smaller than those of the transferring ions in our experiments, for the reaction Equation A1, the limiting convolution current I_l^a is controlled by oxidation of R at Pt|W interface and its expression can be obtained from Equation A3:

$$I_l^a = FA_1 C_R^{W,*} (\pi D_R^W)^{1/2} \tag{A11}$$

Thus, with combination of Equation A3 and Equation A5 when $I = I_l^a/2$, the $E_{1/2}$ (vs. E_{Ref}^{IL}) of the reaction in Equation A1 can be given by

$$E_{1/2}(B^-) = \Delta_W^{Pt}\phi^{\Theta'} + \Delta_{IL}^W\phi_{B^-}^{\Theta'} - f\ln(2\gamma_1 K_1 - t_{A^+}^{IL}) + C_1 \tag{A12}$$

with

$$\left.\begin{array}{l} \gamma_1 = (D^{IL}/D_R^W)^{1/2}, K_1 = (C^{IL,*}/C_R^{W,*}) \\ C_1 = f\ln\left[(D^{IL}/D_{B^-}^W)^{1/2}(2C_O^{W,*}/C_R^{W,*} + \xi)\right] \end{array}\right\} \tag{A13}$$

On the basis of the same principle, we can obtain $E_{1/2}$ of the reaction in Equation A2,

$$E_{1/2}(A^+) = \Delta_W^{Pt}\phi^{\Theta'} + \Delta_{IL}^W\phi_{A^+}^{\Theta'} + f\ln(2\gamma_2 K_2 - t_{B^-}^{IL}) + C_2 \tag{A14}$$

with

$$\left.\begin{array}{l} \gamma_2 = (D^{IL}/D_O^W)^{1/2}, K_2 = (C^{IL,*}/C_O^{W,*}) \\ C_2 = f\ln\left\{(D_{A^+}^W/D^{IL})^{1/2}[\xi/(1 + 2\xi/(C_O^{W,*}/C_R^{W,*}))]\right\} \end{array}\right\} \tag{A15}$$

For the $E_{1/2}$ (X^-) of anion transfer from water to mIL, since more than two ions are located in water, electronmigration in this case is complex. On the basis of our previously simplified consideration [9a], the $E_{1/2}$ (vs. E_{Ref}^{IL}) can be represented by,

$$E_{1/2}(X^-) = \Delta_W^{Pt}\phi^{\Theta'} + \Delta_{IL}^W\phi_{X^-}^{\Theta'} + f\ln\frac{2(D_{X^-}^{IL})^{1/2}C_{X^-}^{W,*}}{(D_O^W)^{1/2}C_O^{W,*}} \tag{A16}$$

where $\Delta_{IL}^W\phi_{X^-}^{\Theta'}$ is the standard transfer potential of X^-. $D_{X^-}^{IL}$ and $C_{X^-}^{W,*}$ are the diffusion coefficients of X^- in mIL and bulk concentrations of X^- in aqueous solution, respectively.

Acknowledgement

References

[1] Z. Samec, V. Marecek, J. Koryta, M. W. Khalil, *J. Electroanal. Chem.* **1977**, *83*, 393.

[2] a) J. A. Campbell, H. H. Girault, *J. Electroanal. Chem.* **1989**, *266*, 465; b) G. Taylor, H. H. J. Girault, *J. Electroanal. Chem.* **1986**, *208*, 179.

[3] a) E. A. de Eulate, D. W. M. Arrigan, *Anal. Chem.* **2012**, *84*, 2505; b) M. D. Scanlon, J. Strutwolf, D. W. M. Arrigan, *Phys. Chem. Chem. Phys.* **2010**, *12*, 10040; c) R. Zazpe, C. Hibert, J. O'Brien, Y. H. Lanyon, D. W. M. Arrigan, *Lab on a Chip* **2007**, *7*, 1732.

[4] P. Jing, M. Q. Zhang, H. Hu, X. D. Xu, Z. W. Liang, B. Li, L. Shen, S. B. Xie, C. M. Pereira, Y. H. Shao, *Angew. Chem. Int. Ed.* **2006**, *45*, 6861.

[5] Y. X. Wang, T. Kakiuchi, Y. Yasui, M. V. Mirkin, *J. Am. Chem. Soc.* **2010**, *132*, 16945.

[6] C. N. Shi, F. C. Anson, *J. Phys. Chem. B* **1998**, *102*, 9850.

[7] S. Ulmeanu, H. J. Lee, D. J. Fermin, H. H. Girault, Y. H. Shao, *Electrochem. Commun.* **2001**, *3*, 219.

[8] M. T. Alam, M. Sohail, R. De Macro, *Electrochem. Commun.* **2012**, *19*, 142.

[9] a) M. Zhou, S. Y. Gan, L. J. Zhong, B. Su, L. Niu, *Anal. Chem.* **2010**, *82*, 7857; b) L. J. Zhong, M. Zhou, S. Y. Gan, Y. Bao, X. D. Dong, L. Niu, L. P. Guo, *Electrochem. Commun.* **2011**, *13*, 221;

[10] C. E. Banks, T. J. Davies, R. G. Evans, G. Hignett, A. J. Wain, N. S. Lawrence, J. D. Wadhawan, F. Marken, R. G. Compton, *Phys. Chem. Chem. Phys.* **2003**, *5*, 40539.

[11] a) R. Gulaboski, V. Mirceski, C. M. Pereira, M. Cordeiro, A. F. Silva, F. Quentel, M. L'Her, M. Lovric, *Langmuir* **2006**, *22*, 3404; b) V. Mirceski, F. Quentel, M. L'Her, A. Pondaven, *Electrochem. Commun.* **2005**, *7*, 1122; c) V. Mirceski, F. Quentel, M. L'Her, F. Scholz, *J. Electroanal. Chem.* **2006**, *586*, 86; d) F. Quentel, V. Mirceski, C. Elleouet, M. L'Her, *J. Phys. Chem. C* **2008**, *112*, 15553; e) F. Quentel, V. Mirceski, M. L'Her, *Anal. Chem.* **2005**, *77*, 1940.

[12] a) F. Quentel, V. Mirceski, M. L'Her, *J. Phys. Chem. B* **2005**, *109*, 1262; b) F. Scholz, R. Gulaboski, *ChemPhysChem* **2005**, *6*, 16; c) F. Scholz, S. Komorsky-Lovric, M. Lovric, *Electrochem. Commun.* **2000**, *2*, 112; d) G. Bouchard, A. Galland, P. A. Carrupt, R. Gulaboski, V. Mirceski, F. Scholz, H. H. Girault, *Phys. Chem. Chem. Phys.* **2003**, *5*, 3748.

[13] K. Charreteur, F. Quentel, C. Elleouet, M. L'Her, *Anal. Chem.* **2008**, *80*, 5065.

[14] a) R. Ishimatsu, N. Nishi, T. Kakiuchi, *Langmuir* **2007**, *23*, 7608; b) R. Ishimatsu, F. Shigematsu, T. Hakuto, N. Nishi, T. Kakiuchi, *Langmuir* **2007**, *23*, 925; c) Y. Yasui, Y. Kitazumi, N. Nishi, T. Kakiuchi, *J. Phys. Chem. B* **2010**, *114*, 11141.

[15] a) T. Kakiuchi, Y. Yasui, Y. Kitazumi, N. Nishi, *ChemPhysChem* **2010**, *11*, 2912; b) Y. Yasui, Y. Kitazumi, R. Ishimatsu, N. Nishi, T. Kakiuchi, *J. Phys. Chem. B* **2009**, *113*, 3273; c) Y. Yasui, Y. Kitazumi, H. Mizunuma, N. Nishi, T. Kakiuchi, *Electrochem. Commun.* **2010**, *12*, 1479.

[16] T. Goto, K. Maeda, Y. Yoshida, *Langmuir* **2005**, *21*, 11788.

[17] A. E. Visser, R. P. Swatloski, S. T. Griffin, D. H. Hartman, R. D. Rogers, *Sep. Sci. Technol.* **2001**, *36*, 785.

[18] A. Berthod, M. J. Ruiz-Angel, S. Huguet, *Anal. Chem.* **2005**, *77*, 4071.

[19] M. Moniruzzaman, N. Kamiya, A. Goto, *Langmuir* **2009**, *25*, 977.

[20] a) T. Kakiuchi, T. Yoshimatsu, *Bull. Chem. Soc. Jpn.* **2006**, *79*, 1017; b) T. Kakiuchi, T. Yoshimatsu, N. Nishi, *Anal. Chem.* **2007**, *79*, 7187; c) M. Shibata, M. Yamanuki, Y. Iwamoto, S. Nomura, T. Kakiuchi, *Anal. Sci.* **2010**, *26*, 1203; d) T. Yoshimatsu, T. Kakiuchi, *Anal. Sci.* **2007**, *23*, 1049.

[21] a) B. M. Quinn, Z. F. Ding, R. Moulton, A. J. Bard, *Langmuir* **2002**, *18*, 1734. b) N. Tsujioka, S. Imakura, N. Nishi, T. Kakiuchi, *Anal. Sci.* **2006**, *22*, 667.

[22] D. S. Silvester, D. W. M. Arrigan, *Electrochem. Commun.* **2011**, *13*, 477.

[23] BEHSS: bis(2-ethylhexyl)sulfosuccinate; TPFB: tetrakis-[3,5-bis(trifluoromethyl)Phenl]borate. $C_nSO_3^-$: alkanesulfonate anion; $C_7F_{15}COO^-$: pentadecafluorooctanoate anion; $C_8mimC_2C_2N$: 1-octyl-3-methylimidazolium bis(trifluoroethylsulfonyl)imide; [H3DA][TPFB20]: tri(hexyl)tetradecylammonium tetrakis(pentafluorophenyl)borate.

[24] a) R. Ishimatsu, N. Nishi, T. Kakiuchi, *Chem. Lett.* **2007**, *36*, 1166; b) N. Nishi, T. Kawakami, F. Shigematsu, M. Yamamoto, T. Kakiuchi, *Green Chem.* **2006**, *8*, 349; c) A. D. Ballantyne, A. K. Brisdon, R. A. W. Dryfe, *Chem. Commun.* **2008**, 4980.

[25] a) N. Nishi, S. Imakura, T. Kakiuchi, *Anal. Chem.* **2006**, *78*, 2726; b) N. Nishi, H. Murakami, S. Imakura, T. Kakiuchi, *Anal. Chem.* **2006**, *78*, 5805.

[26] a) S. M. Ulmeanu, H. Jensen, Z. Samec, G. Bouchard, P. A. Carrupt, H. H. Girault, *J. Electroanal. Chem.* **2002**, *530*, 10; b) J. Langmaier, Z. Samec, *Electrochem. Commun.* **2007**, *9*, 2633; c) J. Langmaier, Z. Samec, *Anal. Chem.* **2009**, *81*, 6382.

[27] a) Z. Same, A. Trojanek, J. Langmaier, E. Samcova, *J. Electroanal. Chem.* **2000**, *481*, 1; b) A. Molina, J. A. Ortuno, C. Serna, E. Torralba, *Phys. Chem. Chem. Phys.* **2010**, *12*, 13296; c) A. Molina, J. A. Ortuno, C. Serna, E. Torralba, J. Gonzalez, *Electroanalysis* **2010**, *22*, 1634; d) A. Molina, C. Serna, J. Gonzalez, J. A. Ortuno, E. Torralba, *Phys. Chem. Chem. Phys.* **2009**, *11*, 1159.

[28] T. Kakiuchi, *Anal. Chem.* **2007**, *79*, 6442.

[29] a) T. Kakiuchi, M. Chiba, N. Sezaki, M. Nakagawa, *Electrochem. Commun.* **2002**, *4*, 701; b) T. Kakiuchi, N. Nishi, T. Kasahara, M. Chiba, *Chemphyschem* **2003**, *4*, 179; c) T. Kasahara, N. Nishi, M. Yamamoto, T. Kakiuchi, *Langmuir* **2004**, *20*, 875; d) A. Berduque, M. D. Scanlon, C. J. Collins, D. W. M. Arrigan, *Langmuir* **2007**, *23*, 7356.

[30] a) T. Kakiuchi, *J. Electroanal. Chem.* **2001**, *496*, 137; b) T. Kakiuchi, *J. Electroanal. Chem.* **2002**, *536*, 63; c) T. Kakiuchi, *J. Electroanal. Chem.* **2004**, *569*, 287; d) Y. Kitazumi, T. Kakiuchi, *J. Phys.: Condens. Matter* **2007**, *19*, 375104; e) Y. Kitazumi, T. Kakiuchi, *Langmuir* **2009**, *25*, 8062; f) Y. Kitazumi, T. Kakiuchi, *J. Electroanal. Chem.* **2010**, *648*, 8.

[31] L. I. Daikhin, M. Urbakh, *J. Chem. Phys.* **2008**, *128*, 014706.

[32] T. Kakiuchi, F. Shigematsu, T. Kasahara, N. Nishi, M. Yamamoto, *Phys. Chem. Chem. Phys.* **2004**, *6*, 4445.

[33] a) T. Kakiuchi, N. Tsujioka, *Electrochem. Commun.* **2003**, *5*, 253; b) T. Kakiuchi, N. Tsujioka, S. Kurita, Y. Iwami, *Electrochem. Commun.* **2003**, *5*, 159.

[34] T. Kakiuchi, N. Tsujioka, *J. Electroanal. Chem.* **2007**, *599*, 209.

[35] J. Langmaier, A. Trojanek, Z. Samec, *Electroanalysis* **2009**, *21*, 1977.

These are not the final page numbers! ↗↗

[36] a) F. O. Laforge, T. Kakiuchi, F. Shigematsu, M. V. Mirkin, *J. Am. Chem. Soc.* **2004**, *126*, 15380; b) F. O. Laforge, T. Kakiuchi, F. Shigematsu, M. V. Mirkin, *Langmuir* **2006**, *22*, 10705.

[37] a) C. N. Shi, F. C. Anson, *J. Phys. Chem. B* **1999**, *103*, 6283; b) T. Kakiuchi, *Anal. Chem.* **1996**, *68*, 3658.

[38] Y. F. Cheng, D. J. Schiffrin, *J. Electroanal. Chem.* **1997**, *429*, 37.

[39] a) J. Niedziolka, E. Rozniecka, J. Stafiej, J. Sirieix-Plenet, L. Gaillon, D. di Caprio, M. Opallo, *Chem. Commun.* **2005**, 2954; b) E. Rozniecka, G. Shul, J. Sirieix-Plenet, L. Gaillon, M. Opallo, *Electrochem. Commun.* **2005**, *7*, 299; c) E. Rozniecka, J. Niedziolka, J. Sirieix-Plenet, L. Gaillon, M. A. Murphy, F. Marken, M. Opallo, *J. Electroanal. Chem.* **2006**, *587*, 133; d) G. Shul, J. Sirieix-Plenet, L. Gaillon, M. Opallo, *Electrochem. Commun.* **2006**, *8*, 1111.

[40] K. Tanaka, N. Nishi, T. Kakiuchi, *Anal. Sci.* **2004**, *20*, 1553.

[41] T. Kakiuchi; M. Senda, *Collect. Czech. Chem. Commun.* **1991**, *56*, 112.

⭦⭦ These are not the final page numbers!